JULY 07, 2020
CONFERENCE
ONLINE

Graphene Online &2DM
Fundamental Research Insights

GO 2020

Topological Aharonov-Bohm Interferometers Defined By Inhomogeneous Electric Field In Silicene

Bartłomiej Rzeszotarski, Alina Mreńca-Kolasińska, and Bartłomiej Szafran

AGH University of Science and Technology, Faculty of Physics and Applied Computer Science
al. Mickiewicza 30, 30-059 Kraków, Poland

AGH

Faculty of Physics and Applied Computer Science

Introduction

We study topologically protected currents as a source of Aharonov-Bohm oscillations in clean systems in silicene [1]. Chiral channels [2,3] in the system are formed by flips of the electric potential perpendicular to the structure [4,5]. In our calculations we define four terminal system in quantum ring shape.

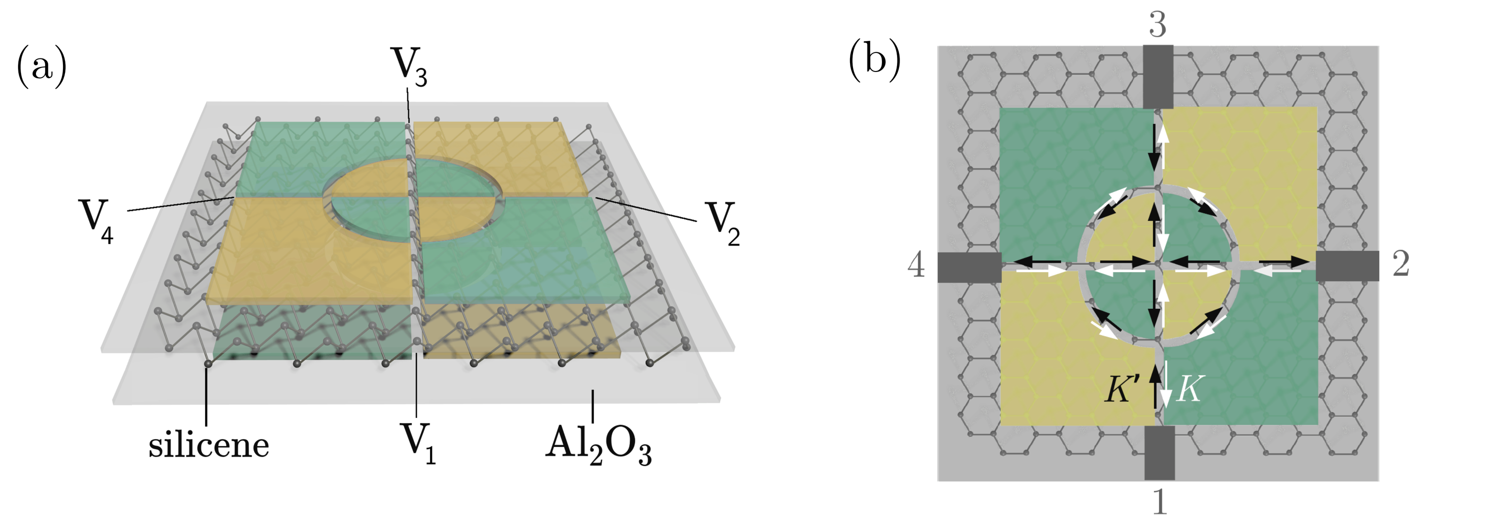

FIG. 1. (a) Scheme of the silicene monolayer between bottom and top gates. Positive potential V_G is put on the green gates, and negative $-V_G$ on the yellow gates. (b) Top view of the system with leads numeration. White (black) arrows denote for the directions of K (K') valley protected charge currents within each channel defined by gate interfaces

Theory

In our calculations we use the atomistic tight-binding Hamiltionian

$$H = -t \sum_{\langle n,m \rangle} (p_{nm} c_n^\dagger c_m + h.c.) + \sum_n V(\mathbf{r}_n) c_n^\dagger c_n \, . \quad (1)$$

The quantum ring with the chiral channels is formed by the electric field induced by the split top and bottom gates. We model the electric potential as

$$V_A = \frac{8V_G}{\pi^3} \arctan\left(\frac{x}{\lambda}\right) \arctan\left(\frac{y}{\lambda}\right) \arctan\left(\frac{\mathcal{R}-r}{\lambda}\right), \quad (2)$$

where V_G is the gate potential, and λ is the parameter responsible for the inversion length. For symmetric gating the potential on the B sublattice is opposite $V_B(r) = -V_A(r)$. The inversion of the field creates a topologically protected conducting channel. The current injected from terminal zero-line 1 can be directed to either terminal 2 or terminal 4. In terminal 3 there is no K' valley state that carries the electron flow up, away from the ring (Fig. 2).

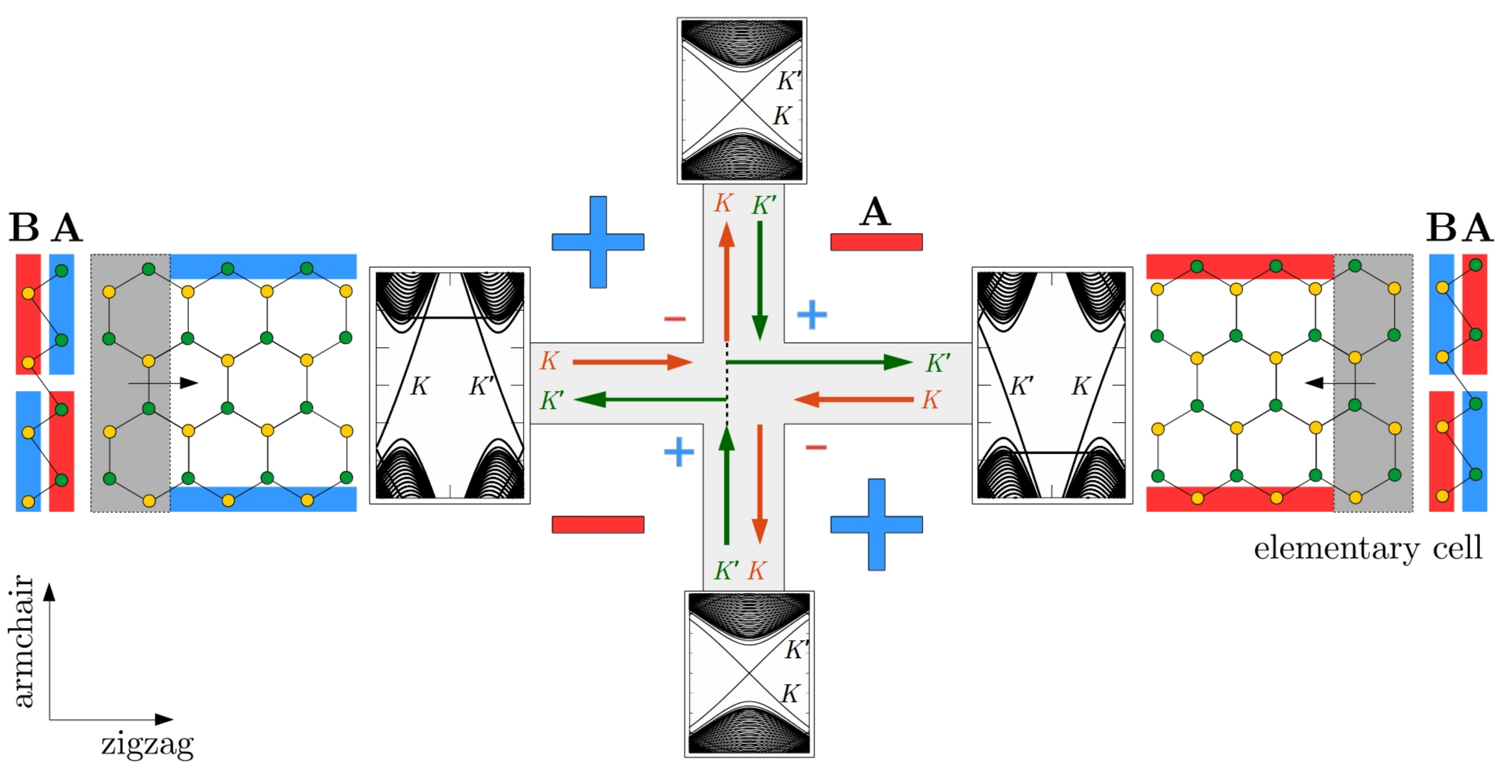

FIG. 2. Sketch of the four-terminal crossing channels defined by flips of the electric potential. We mark negative potential $-V_G$ (red, "–" symbol) and positive V_G (blue, "+" symbol), for both the A (upper) and B (lower) sublattice. Red (green) arrows indicate the orientation of the K (K') currents in the channel that are associated with a specific valley marked in the band structures for each lead.

Results and discussion

The current is evenly distributed from terminal 1 to the left and the right leads [Fig 3(a,c)] while for stationary points of conductance A (B) [Fig 4(a)] and for other cases the current mostly localizes around quarters of the ring [Fig 3(b,d)]. Two different configurations of resistance measurement are proposed: (i) in straight line (e.g. 3→1) and (ii) with current probes plugged to two nearest leads (e.g. 4→1), as presented in Fig. 3(e) and 3(f), respectively.

Oscillations of the conductance [Fig. 4(a)] and resistance measurement [Fig. 4(b)] in external magnetic field are related to the current confinement at quarters of the ring. By taking the Fourier transform of the resistance R for magnetic field B range from 0 to 40 T we can distinguish four characteristic peaks [Fig. 4(c)]. The period of these oscillations agree with Aharonov-Bohm interference at n/4 (n=1,2,3,4) of the area of the circle.

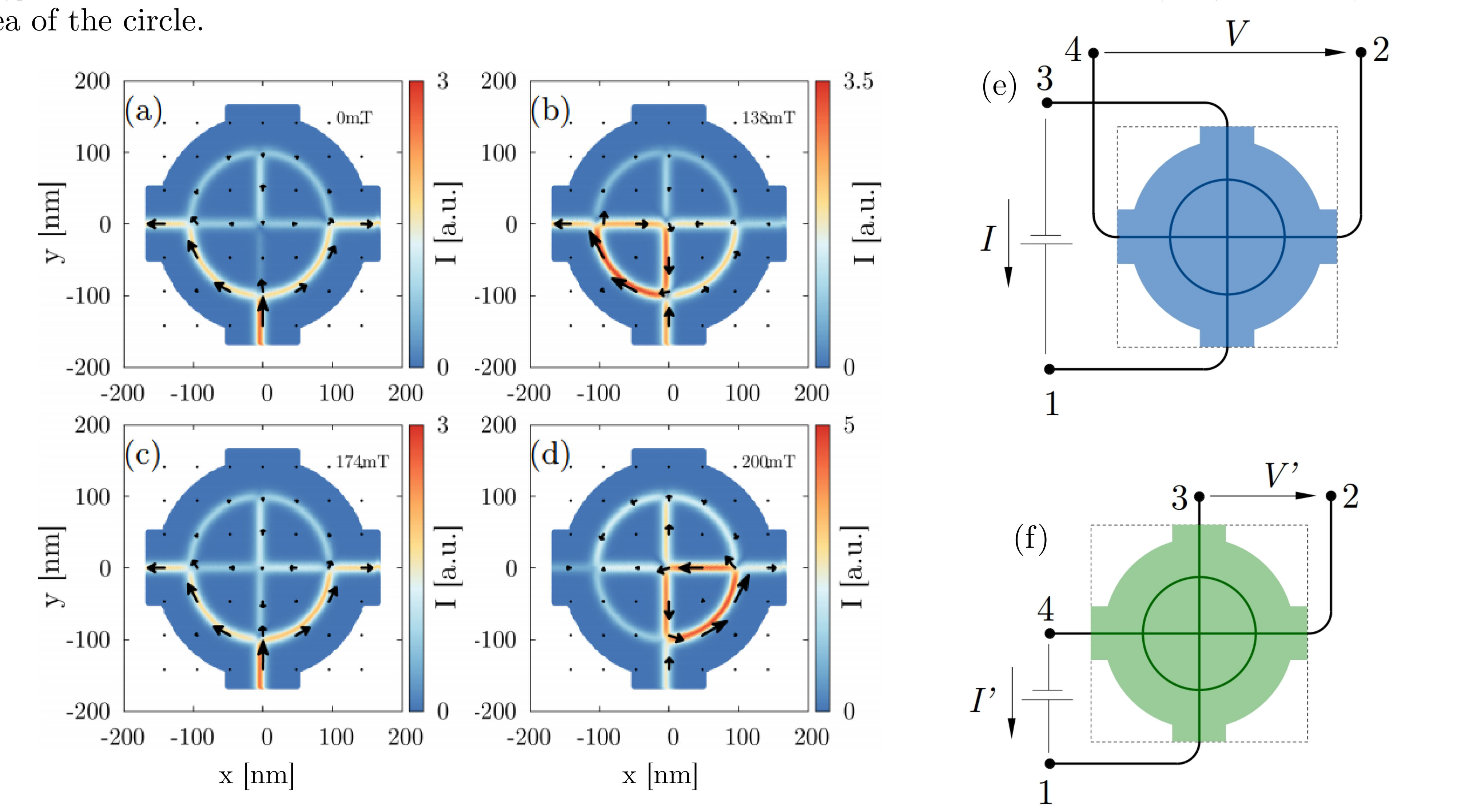

FIG. 3. (a-d) Current distribution maps for specific magnetic field magnitudes. For each map the color indicates the averaged current amplitude, while the arrows indicate the direction of this current. (e,f) Schemes of the experimental resistance measurement configuration: for the current flow between opposite and neighbor leads, respectively. In both configurations the voltage associated to the third lead is set to 0.

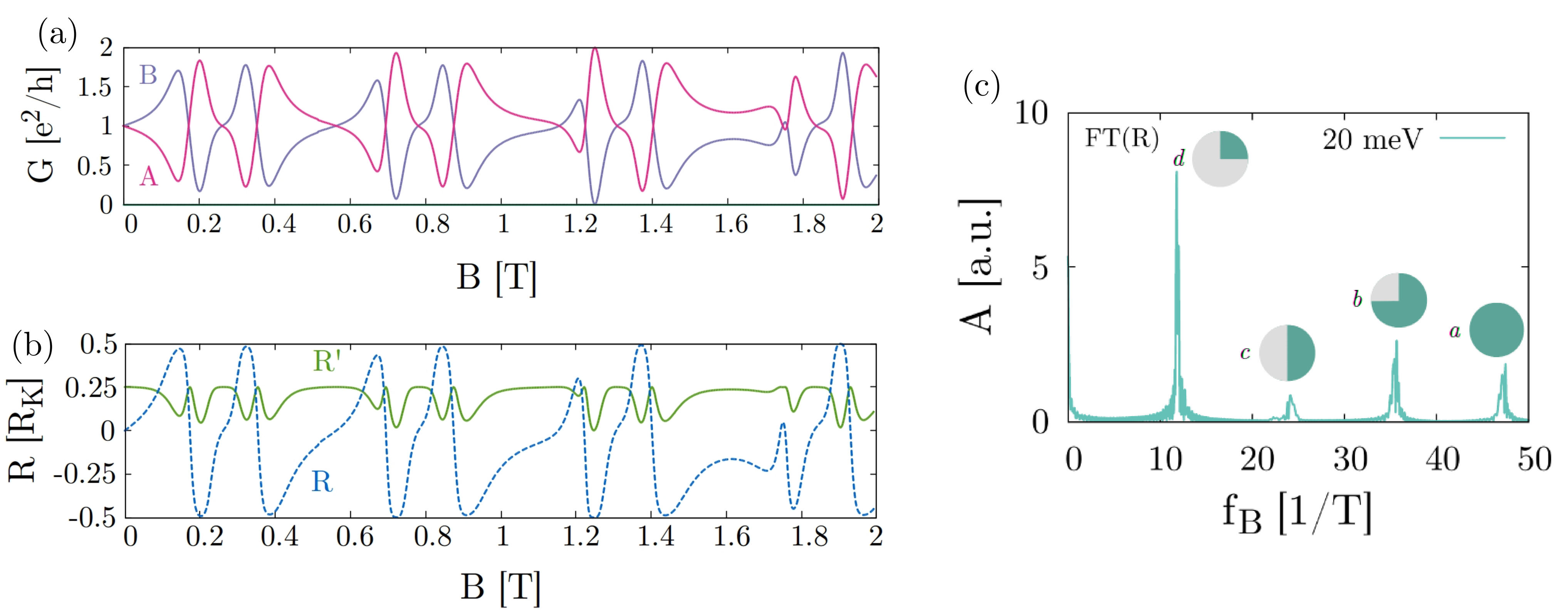

FIG. 4. (a) Conductance plot for the system in external magnetic field at fixed Fermi level, where $A = G_{14} = G_{21} = G_{32} = G_{43}$, and $B = G_{41} = G_{12} = G_{23} = G_{34}$. (b) Resistance R' for the case in Fig. 3(f) and R [case in Fig. 3(e)] in units of von Klitzing constant R_K. (c) Fourier transform of R(B). Input magnetic field range B was set to [0:40] T. Inset icons indicate the area encircled by the currents to produce Aharonov-Bohm periodicity corresponding to the peaks *a-d*.

Acknowledgments

B.R. is supported by Polish government budget for science in 2017-2021 as a research project under the program "Diamentowy Grant" (Grant No. 0045/DIA/2017/46), by the EU Project POWR.03.02.00-00-I004/16 and NCN grant UMO2019/32T/ST3/00044. The calculations were performed on PL-Grid Infrastructure on Rackserver Zeus at ACK-AGH Cyfronet.

CONTACT PERSON

Bartłomiej Rzeszotarski
rzeszotarski@fis.agh.edu.pl

REFERENCES

https://doi.org/10.1103/PhysRevB.101.115308

[1] B. Aufray, A. Kara, S. Vizzini, et al. , Applied Physics Letters 96, 183102 (2010)
[2] W. Yao, S. Yang, , and Q. Niu, Phys. Rev. Lett. 102, 096801 (2009)
[3] M. Katsnelson, K. Novoselov, and A. K. Geim, Nature Phys. 2, 620 (2006)
[4] M. Ezawa, New Journal of Physics 14, 033003 (2012)
[5] B. Szafran, B. Rzeszotarski, and A. Mreńca-Kolasińska, Phys. Rev. B 100, 085306 (2019)

Graphene Online &2DM
Fundamental Research Insights
GO 2020